CrystEngComm

Accepted Manuscript

ROYAL SOCIETY OF CHEMISTRY

www.rsc.org/crystengcomm

Cite this: DOI: 10.1039/c0xx00000x

www.rsc.org/xxxxxx

ARTICLE TYPE

Effects of CTAB concentrations on properties of electrodeposited cadmium telluride films

Qian Li,[a] Kailin Chi,[a] Yannan Mu,[a,b] Wenjiao Zhang,[a] Pin Lv,[a] Liying Zhou,[a] Haibin Yang*,[a] Wuyou Fu[a]

Received (in XXX, XXX) Xth XXXXXXXXX 200X, Accepted Xth XXXXXXXXX 200X

DOI: 10.1039/b000000x

The effects of cetyltrimethylammonium bromide (CTAB) concentrations on the properties of electrochemical deposited cadmium telluride films have been investigated using scanning electron microscopy (SEM), energy-dispersive X-ray (EDX), X-ray diffraction (XRD), and photoelectrochemical measurements. The results show that CTAB concentrations play a very important role in directing the morphology evolution of thick films from cabbage-shaped CdTe array to high denser nanoneedle structure. Various CdTe structures can be obtained by changing CTAB concentrations in the electrolyte. Meantime, it is observed that the Te/Cd ratio of the as-deposited thin film decreased with the increase of CTAB concentration. When CTAB concentrations are 0.02 M, the composition of CdTe film is near stoichiometric and the amount of Te is excessive. Growth mechanisms for shape-selective CdTe synthesis were proposed based on these results. In addition, we find the device based on the aligned cabbage-shaped CdTe array-on-Ni configuration prepared at 0.02 M CTAB demonstrates excellent photoelectrical properties, which is ascribed to the large absorption coefficient of the material and also suggests good electronic structure quality of the cabbage-shaped rods.

Introduction

Solar power is a promising candidate as a sustainable energy supply. As a result, much effort has been put into developing inexpensive materials and architectures that reduce cost and/or increase efficiency[1-4]. In the search for low-cost alternatives to monocrystalline silicon, thin film p-CdTe:n-CdS photovoltaic cells prepared by electrodeposition[5-8] are reaching the point where commercial exploitation is feasible. For optimal conversion efficiency, solar devices must absorb most of the incident light and the resulting charges must be utilized before they recombine[9-10]. CdTe thin film has an optical band gap which is very suitable for its use as an absorption layer in solar cell structures[11-12], so the growth of the high quality CdTe nanocrystalline thin films is important.

The best CdTe solar cells have the following layered structure: glass, transparent conducting oxide front contact (usually indium tin oxide), CdS window, CdTe absorber, and back contact. But these same cells have problems with glass breakage during manufacture since the cells must be heated to near the softening point of glass. Furthermore, the poor thermal conductivity of glass contributes to low panel yields because of temperature variations across a panel during anneal. Thin film solar cells on metal foils can solve most of these problems as well as reduce weight for space applications, while holding promise for more efficient and less expensive panels. Therefore, more and more researchers are concentrating on fabricating high-quality CdTe film on metal foils. Up to now, various CdTe nanostructures have been prepared by many methods including close space sublimation (CSS)[13], thermal evaporation[14], hydrothermal, solution chemical[15], template-assisted approaches[16] and electrochemical deposition[17]. Among these methods, electrodeposition techniques gain an advantage over other high temperature processes by simplicity, large scale, low cost and low temperature. In recent years, the controlled growth of CdTe nanostructures by low-temperature techniques has become the focus of world attention. Therefore, many efforts have been made to give insight into the effects of process parameters on the growth behavior of CdTe semiconductor materials. At present, it has been proved that the growth of one-dimensional CdTe can be manipulated by adjusting deposition voltage during electrodeposition.[18] This is a fast, simple, and reproducible method which does not require any template, catalyst, or surfactant but can control the morphology of CdTe. In addition, it is widely accepted that one of the promising and popular strategies of shape control is to select carefully an appropriate organic additive with functional groups that selectively adheres to crystal facet, leading to the morphological modification of the crystals.[19-21] Among a variety of organic additives, cetyltrimethyl ammonium bromide (CTAB) is one of the most common and important organic molecules that has been used extensively as the stabilizer and structure-directing agent to control the nucleation, growth and alignment of crystals[22]. For example, Qian and coworkers reported the wire-like and flower-like ZnO nanostructures were easily prepared using a CTAB structure-directing [23].

Herein, we aim to explore the effects of surfactant CTAB concentration on the CdTe films deposited during electrochemical deposition and demonstrate the morphology evolution of films

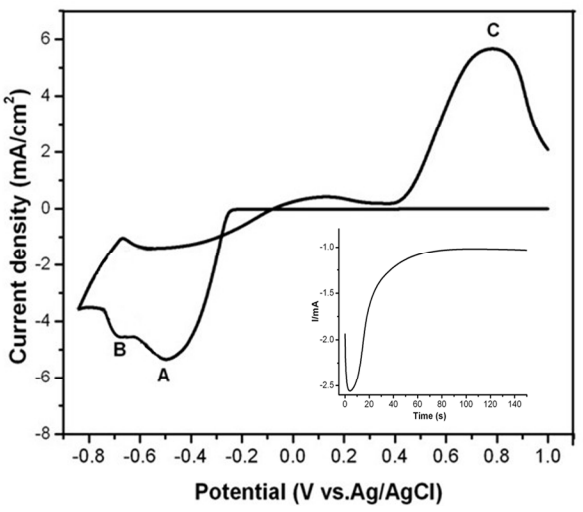

Fig. 1 Cyclic voltammograms of 0.05 M Cd^{2+}+0.006 M TeO_3^{2-} at room temperature, CTAB =0.02 M, and scan rate=100 mV/s. The lower inset shows the change in current density during potentiostatic electrodeposition at -0.50 V within the first 140 s.

from cabbage-shaped rod array to nanoneedle-like structure. Our electrodeposition method works at a room temperature and has a short reaction time (60 min). Also, it does not require any template or catalyst. Various CdTe crystal architectures with simple or complex can be constructed using this facile and fast method. In addition, Cd and Te contents and photovoltaic performance of as-deposited film influenced by CTAB concentration are researched. The possible origins are discussed as well. The results of this research allow us to propose growth mechanisms for shape-selective CdTe synthesis.

In addition, we find that CdTe cabbage-shaped rods array occur obviously when CTAB concentration approaches to 0.02 M, this structure exhibite an improved open circuit voltage, short circuit current, fill factor, and consequently an overall enhancement of the power conversion efficiency than CdTe traditional nanorod arrays, so this structural may be beneficial for the potential applications in solar cells.

Experimental Section

The electrodeposition of CdTe was performed at room temperature in a three electrode electrochemical cell with the substrate (Ni) as the cathode, a graphite plate as the counter electrode and a saturated silver/silver chloride (Ag/AgCl) electrode as the reference electrode. Before performing the experiment, the Ni substrates had been pretreat by an ultrasonic cleaner for 20 min in isopropanol, acetone, anhydrous ethanol and double-distilled water respectively. In this paper all the potentials are quoted versus Ag/AgCl. For all the experiments presented here the electrolytic solution was prepared by dissolving 0.05 M of Cd ions (the precursor salt is $CdSO_4 \cdot 8/3H_2O$) in a saturated solution of Te ions (Na_2TeO_3, about 0.006 M). The deposition bath typically contained 0.03 M Na_2SO_4, which acts, among other roles as a supporting electrolyte. CTAB (0.02, 0.03, 0.04 or 0.05 M) was added to electrolyte directly at room temperature. The pH of the electrolyte was adjusted by adding H_2SO_4. After deposition, samples were washed with distilled water to remove excess telluride from the surface.

The microstructure of the samples were examined using field-emission scanning electron microscopy JEOLJXA-8200 (SEM). The structural properties of the as prepared product were analyzed using a Rigaku D / max-2500 X-ray diffractometer with Cu K_α radiation (λ=1.5418 Å). The optoelectronic properties were investigated using a conventional three-electrode system made of quartz cell linked with the electrochemical workstation (CH Instruments model CHI601C). The CHI electrochemical workstation was used to measure the illuminated current at a scan rate of 10 mV/s. The sunlight was calibrated by a 500 W xenon lamp (Spectra Physics) and the light intensity was simulated with a laser power meter (BG26M92C, Midwest Group), amount to light at 100 mW/cm^2.

Results and discussion

Electrochemical behavior

The cathodic polarization behavior in the electroplating bath often yields useful information regarding the onset potential of cathodic process, its rate and the existence of a transport limitation. A typical voltammogramme recorded in an aqueous bath of composition 0.05 M $CdSO_4$, 0.006 M TeO_3^{2-} and CTAB (0.02 M) has been shown in Fig. 1.

The voltammogramme were recorded at the scan rate of 100 mVs^{-1}, on Ni substrate working electrode. In the cyclic voltammogram of Cd^{2+} and Te^{4+}, as shown in Fig. 1, The first cathodic onset observed at -0.50 V (vs Ag/AgCl) corresponds to the cathodic reduction of the Te ions. With increasing cathodic scan; another sharp cathodic onset was recorded at −0.83 V, implying the initiation of a new cathodic process, two cathode current peaks appear at -0.50 and -0.70 V, which respectively correspond to the reductions of TeO_3^{2-} to elemental Te and Te to Te^{2-} according to[24-25]:

$$TeO_3^{2-} + 3H_2O + 4e \rightarrow Te^0 + 6OH^- \quad (1)$$

$$Te^0 + Cd^{2+} + 2e \rightarrow CdTe \quad (2)$$

$$TeO_3^{2-} + Cd^{2+} + 3H_2O + 6e \rightarrow CdTe + 6OH^- \quad (3)$$

Therefore, the deposition of CdTe on Ni substrates might be formed at a fixed potential of -0.50 V versus Ag/AgCl electrode to promote the one-step reaction of TeO_3^{2-} and Cd^{2+} shown in eq 3.

The lower inset of Fig. 1 shows the change of cathodic current density with time during the potentiostatic electrodeposition at a potential of -0.50 V versus Ag/AgCl for the first 150 s. It was observed that the cathodic current density decrease quickly at initial time and increase gradually. During electrodeposition, first, all the current densities decrease abruptly due to nucleation on the substrate surface. After the attainment of uniform nucleation on the entire surface, the current density became constant and the film growth began. After 25–30 min, a CdTe layer was deposited.

Structural characterization

Fig. 2 shows the X-ray diffraction patterns of CdTe thin films electrodeposited using different CTAB concentration. All the diffraction peaks can be assigned to zinc-blende CdTe with the exception of some peaks attributed to Ni substrate. The

characteristic zinc blende planes of (111), (220) and (311) locat-ing at 23.98, 39.70 and 49.90° in the 2θ range of 20 to 80° for CdTe have been observed. The (111) direction is obviously much more intensified than other directions, which suggests that the films grow preferentially oriented along the (111) direction. It can be observed that only slight changes of intensity occur in the patterns of XRD with the various CTAB concentration, and the samples keep the characteristic peaks of CdTe intact, which indicates that the changes of surfactant concentrations as modifier does not significantly affect the perfection of the CdTe crystals.

Table 1
Atomic percent of as-prepared films at various CTAB concentrations.

CTAB (M)	Te(%)	Cd(%)	Te/Cd
0.02	57.6±1	42.1±1	1.37±0.01
0.03	54.3±1	43.1±1	1.26±0.01
0.04	46.2±1	53.1±1	0.88±0.01
0.05	41.5±1	60.5±1	0.69±0.01

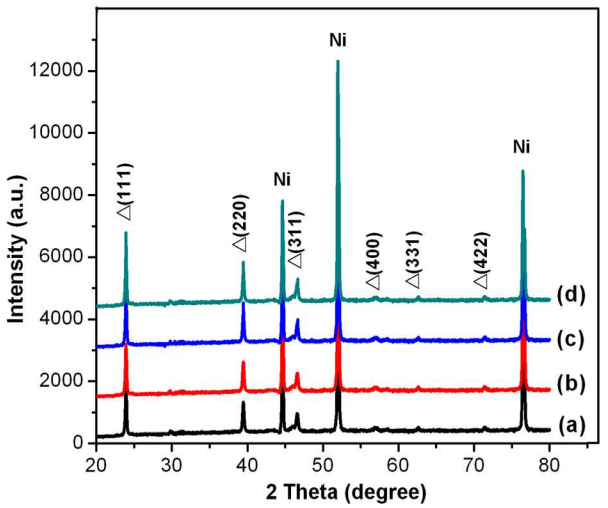

Fig. 2 XRD patterns of the as-prepared CdTe films synthesized at various CTAB concentrations (a) 0.02 M, (b) 0.03 M, (c) 0.04 M, (d) 0.05 M at room temperature for 1 h. The standard diffraction patterns of CdTe are shown by triangles.

In order to further explore the composition of CdTe film that influenced by CTAB concentration, a compositional analysis for the as-deposited CdTe films was carried out using EDAX, and the results of the same are listed in Table 1. These data indicate that the increase of CTAB concentration results in the increase of cadmium content and meantime decrease of tellurium content of CdTe films. It is observed that the Te/Cd ratio of the as-deposited thin film is 1.37 for 0.02 M CTAB, when surfactant concentration increased to 0.05 M, the Cd and Te contents of the film are almost equal, indicating that the composition of a CdTe film is near stoichiometric and the amount of excess Te is very small. It was shown that the film deposited from Te-rich to Cd-rich with CTAB concentration increase.

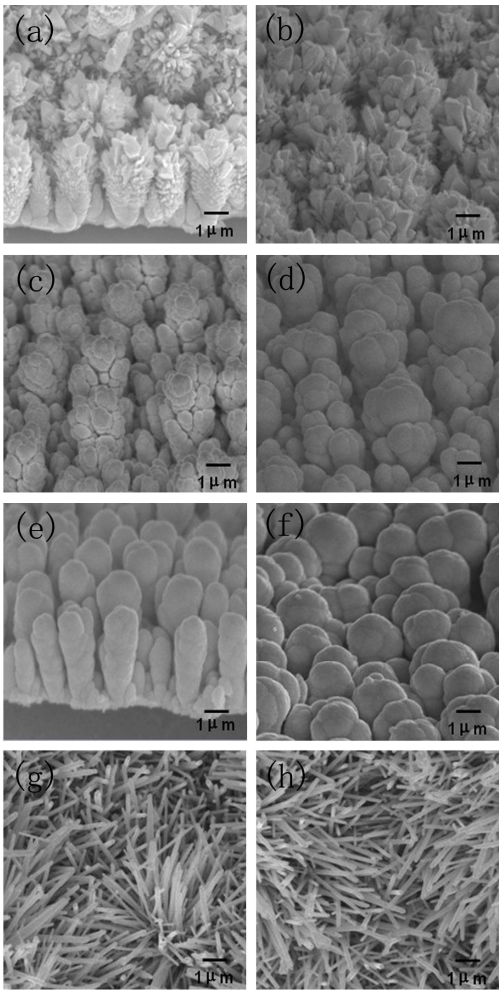

Fig. 3 SEM images of the as-prepared films at a tilted angle of 60 ° (a, c, e, g) and top view (b, d, f, h) synthesized at various CTAB concentrations: (a,b) 0.02 M, (c,d) 0.03 M, (e,f) 0.04 M, (g,h) 0.05 M at room temperature for 1 h.

As we know, electrodeposition of CdTe layer can be devided into two stages. The first stage mainly represent as the continued reduction of TeO_3^{2-} ion, after a sufficient amount of tellurium produced, the electrodeposition process gradually entered into the second stage, performed as Cd and Te deposited together.

Surfactant CTAB can hinder the electron transfer both process of TeO_3^{2-} and Cd^{2+} ions in electrolyte in the same time. Meantime, it can promote the adsorption and desorption of Cd^{2+} ions, between the two, the adsorption of Cd^{2+} ions is major and more significant. But on the whole, the effect of CTAB on the restraining of reduction reaction of the TeO_3^{2-} is much stronger than that of the reaction of Cd^{2+} ions reduced to Cd. In other words, CTAB only has a little effect on the Cd^{2+} ion compared with TeO_3^{2-}. Therefore, with increase of the concentrations of CTAB, at higher surfactant concentrations, the reduction of TeO_3^{2-} ion is inhibited gradually, cause the decrease of Te atoms contents of CdTe film, and lead to the low content of Te atoms compared with Cd. Consequently, concentrations of surfactant CTAB will effect Cd and Te atoms contents of thin

film, and affects the composition of the thin film and Te/Cd ratio.

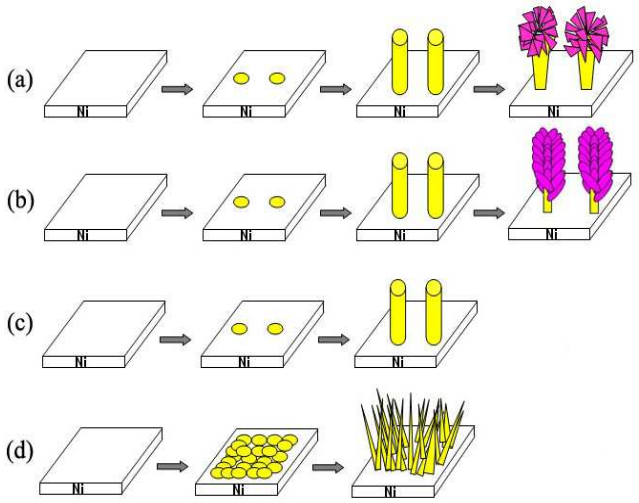

Fig. 4 Schematic diagram of the proposed formation processes of the CdTe samples synthesized at various CTAB concentrations (a) 0.02 M, (b) 0.03 M, (c) 0.04 M, (d) 0.05 M at room temperature for 1 h.

Morphology

CTAB as a cationic surfactant plays an important role in controlling the formation of micro and nano architectures under the template effect. The growth of the certain architecture is associated with the selective interaction of the organic surfactants on certain crystallographic facets to stimulate the crystal growth[26-27]. For better understanding the surfactant CTAB effect, we prepared the CdTe with using varied the surfactant concentration. The FESEM images of the CdTe with different CTAB concentration are shown in Fig. 3.

When CTAB concentrations are 0.02 M, CdTe prepared exhibits the formation of vertically aligned, highly denser CdTe cabbage-shaped CdTe rod arrays with a thickness of about 2 μm tend to grow on the substrate, as shown in Fig. 3(a,b), which may ensure a direct pathway for the photogenerated charge carriers to travel along the longitudinal direction of nanorods with minimum loss, and also may be a promising candidate for applications in solar energy conversion devices. Fig. 3(c) and (d) represent the FESEM micrographs of the prepared CdTe using CTAB with concentrations of 0.03 M, we can see surfactant with concentration of 0.03 M assists CdTe to gain a morphology of high-density CdTe flower-like rod arrays. Whereas with higher CTAB concentration of 0.04 M, CdTe nanostructures are composed of regular aligned and dense microrod array perpendicular to the Ni substrate, which can be observed having an average thickness of 2 μm. Fig. 3(e,f) shows large-scale vertical growth of CdTe microrod arrays has been realized. However, on increasing CTAB concentration further to 0.05 M, as shown in Fig. 3(g,h), which reveal that the products consist of a large quantity of fairly uniform needle-like nanostructures with typical lengths in the range of 2–3 μm, with a diameter of about 30 nm. All of the CdTe nanoneedles show tapered morphology towards their tips. It appears that with the increase of CTAB concentration from 0.02 M to 0.05 M, the tendentious morphology evolution of films from cabbage-shaped CdTe array to high denser nanoneedle-like structure occurs. We speculate

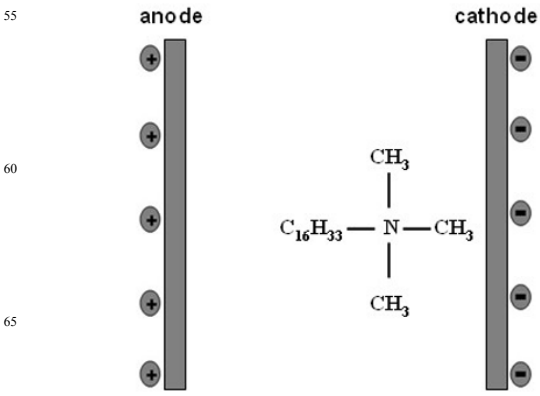

Fig. 5 Schematic illustration of reaction mechanism.

that CTAB play an important role during the formation of CdTe film. However, the interaction mechanism between CdTe and surfactant is complicated and nearly no further works on this line are currently underway to make progress in this respect.

Possible Formation Mechanism

From the above figures, it can be seen that the morphologies of the final products are greatly dependent on the CTAB concentration. It is well known that the CTAB at different concentrations can form into different shapes in aqueous solution[28]. To gain control over the synthesis, it is necessary to understand the mechanism by which the crystal is formed. It is well known that crystal formation in solution can be divided into two stages: crystal nucleation occurs followed by crystal growth occurring from the crystal nuclei.[29] The latter process can also be understood as growth units diffusing in the solution and adsorbing on the nuclei.[30] The formation mechanisms (seen in Fig. 4) may have been proposed to explain the different CdTe morphologies prepared with different surfactant concentration.

Maybe at low surfactant CTAB concentrations (0.02 M), the small CdTe nanoparticles grown at first aggregate easily in order to decrease the energy of the system. CTAB is a cationic surfactant, in the electrodeposition process, under the action of electric field force, its positively charged groups move toward the cathode and gather on the electrode surface, then adsorb on some crystal face. The characteristic of adsorption decreases the surface energy, and change the morphology of crystal. In zinc blende, as the positively charged Cd-(111) polar surface is chemically active and the negatively charged Te-($11\bar{1}$) is relatively inert, this will provide a strong tendency to grow the cabbage-shaped CdTe rods along (111). Moreover, in electrodeposition, the preferred growth not only depends on the crystallography but also on the electrochemical nucleation and growth kinetics. In the control of structural characteristics, nucleation, and growth kinetics, the (111) direction that is parallel to the current direction will be the fastest growth direction among other facets in the CdTe nucleus growth process, and the cabbage-shaped CdTe rod will grow longer along the (111) direction[31]. In low concentration of CTAB, the surface of the nucleate is not well-covered by the adsorbed surfactant molecules. In addition, CTAB is most widely used as cationic

surfactant and the $(CH_3)_4$-N^+ chains of the group is shorter than $C_{16}H_{33}^-$ chains, so $(CH_3)_4$-N^+ may be much closer to surface of the substrate[32], as shown in Fig. 5. This adsorption make the morphology of CdTe thin film divided into two parts, we can see cabbage-shaped CdTe array. A detailed time course study is expected to provide direct evidence for such a speculation. Unfortunately the experiments show the cabbage-shaped CdTe rods are formed quickly, which prevented the direct observation of their detailed formation process. However, the exact mechanism for the morphological control of CdTe film by cationic surfactants is worthy of further investigation.

With higher CTAB concentration of 0.03 M, they may be equivalent to the lyotropic liquid crystal effects, and can be acted as the template of shape controlling, making the morphology of the particals attached to the nanorods changes from the block shape to the smooth spherical. As shown in Fig. 3(c) and (d), the flower-shape CdTe array formed.

When the surfactant CTAB concentration continues to increase, the upper surface of CdTe seeds deposited on Ni substrate are basically covered by the surfactant molecules, so they can be dispersed well, and then grow along a given orientation, with growth orientation along the (111) direction. Finally, rod-like CdTe nanocrystals grow upon. As shown in Fig. 3 (e) and (f), high-density CdTe nanorod arrays vertically aligned in a large area.

At a higher surfactant CTAB concentration (0.05 M), it might be rationalized that all the surface of the nucleate is well-covered by the adsorbed surfactant molecules. When a potential of 0.50 V is applied, all the cations in solution will move towards the cathode, polar part of CTAB will adsorb on the electrode and all the surface of formed CdTe nanoparticles, change the surface energy of different crystal surface of the CdTe nanoparticles, thus affecting the growth of CdTe, so nucleate grow irregularly to all direction, which causes CdTe nanoparticles are no longer growth perpendicular to the electrode surface, therefore, it results in random orientations of the large part of CdTe nanoneedle structure.

In addition, because the CdTe crystals have a face centered cubic structure of which the (111) surface atoms is the most intensive, grains will be firstly grow in the (111) plane, while grow slower in other planes, which can produce preferred orientation. The CdTe prepared on the Ni substrate has a strong textured phenomenon. Though polar part of CTAB will adsorb on the electrode and all the surface of formed CdTe nanoparticles, change the surface energy of different crystal surface of the CdTe nanoparticles, at the same time, difference in surface energy of anisotropic crystalline facets makes the (111) surface of a ZB crystal more active in most of the common cases.

Therefore, the (111) surfaces of the already nucleated CdTe nanocrystals could still serve as accommodating planes, allowing films grow preferentially oriented along the (111) direction. In fact, such mechanism dominates the growth, therefore, the (111) direction of the film is obviously much more intensified than other directions.[33]

However, when surfactant concentration continued to raise much higher, the nucleate is largely covered by the adsorbed surfactant molecules, impaire the direct adsorption of CdTe ions on the nucleate surface, which can lead to poor heterogeneous nucleation sites. Thus a proper surfactant concentration is important for the formation of the morphology of CdTe structure.

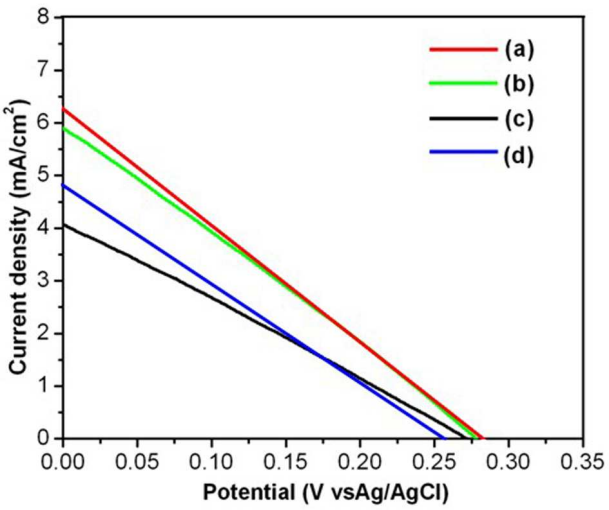

Fig. 6 Photocurrent curve of CdTe films synthesized at various CTAB concentrations (a) 0.02 M, (b) 0.03 M, (c) 0.04 M, (d) 0.05 M at room temperature for 1 h.

Table 2.
Averaged J-E Data of the different samples

CTAB	0.02 M	0.03 M	0.04 M	0.05 M
I_{SC}(mA/cm²)	6.35	5.92	4.12	4.82
V_{oc}(V)	0.29	0.28	0.27	0.25
FF	0.52	0.42	0.25	0.37
η (%)	0.92	0.67	0.28	0.46

*The power of the incident light was ~100 mW/cm²

A proper concentration of surfactant is beneficial to the seeds formed at first to aggregate partially, and then the seeds can grow into branches in every orientation to form different morphology of CdTe films. In a word, it is indicated that a modest concentration of CTAB is required for the heterogeneous nucleation and growth of CdTe crystals but excessive CTAB would considerably impairing heterogeneous nucleation of CdTe.

Photoelectrochemical Measurements

To further investigate the fundamental photovoltaic performance of CdTe films synthesized at various CTAB concentrations, current density versus voltage (J–V) characteristics of different samples were measured under chopped white light with an intensity of ~100 mW/cm^2. The photoelectrochemical assembly consisted of the working electrode, a Pt gauze counter electrode, a Pt wire reference, and a liquid electrolyte, all in a glass cell. The aqueous electrolyte contained 0.2 M NaOH, 0.2 M Na_2S, and 0.2 M S and strongly absorbs at wavelengths <500 nm. This polysulfide (S_n^{2-}) redox mediator is known to form charge-separating junctions with CdTe and to suppress photo-oxidation.[34] Fig. 6 shows the J–V behavior of the samples,

respectively, and the main photovoltaic parameters are listed in Table 2. In present study, the as-prepared CdTe films all show

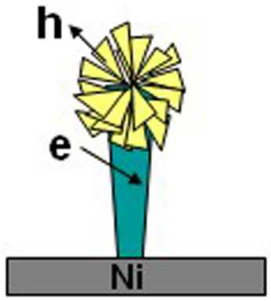

Fig. 7 The electrons and holes transfer schematic diagram: yellow area denotes the space charge region and the blue-green area is the electronic transmission path.

strong photovoltaic performance. The photovoltaic parameters including the short-circuit current density (J_{sc}), the open-circuit voltage (V_{oc}), and the white light power conversion efficiency (η) show a clear dependence on film morphology.

With various of surfactant CTAB concentration, the corresponding J_{sc} and η values decrease from 6.35 to 4.82 mA cm^{-2} and 0.92% to 0.46%, respectively, while the V_{oc} values systematically swing around 0.26 V. The best photovoltaic performance with J_{sc} = 6.35 mA cm^{-2}, V_{oc} = 0.29 V, fill factor (FF) = 0.52, and η=0.92% was obtained when the electrolyte containing 0.02 M CTAB. The results can be rationalized in a way as follows, as shown in Fig. 7, we consider that the morphology of cabbage-shaped CdTe array divided into two parts, the above part with sheet-like structure, which are similar to the leaves of a cabbage can guarantee a large light-receiving area. In addition, the vertical array configuration of the rods on substrate ensures a direct pathway for the photogenerated charge carriers to travel along the longitudinal direction of rods with minimum loss. Consequently, when the sample is irradiated by the simulated solar light, it absorbs more light, and as a result, more electron–hole pairs would separate in the space charge region which is generated at the interface between the cabbage-shaped rod and the polysulphide electrolyte. Electrons are concentrated into the center of the cabbage-shaped CdTe rod to be transported, and holes are transferred to the polysulphide redox electrolyte solution. Overall, by the both effection of the two parts of cabbage-shaped CdTe rod, the whole array has an overall enhancement of the power conversion efficiency compared with other samples. Although the Ni/cabbage-shaped CdTe array/polysulphide junction is an intricate system, it can be a benchmarking basis that achieves the purposes of power output characteristics. As seen from the results of energy conversion efficiency, there is still much room for improvement. This structure would be beneficial in the application of solar cells as the submicrometer sized diameter would enhance the cell photovoltaic parameters.

In this study, it has been observed that the cabbage-shaped CdTe array has an enhanced short circuit current and open circuit voltage compared with traditional CdTe nanorod arrays, it shows the potential in solar energy conversion devices and the excellent photovoltaic performance. The characterization of the cabbage-shaped CdTe array half-cell photoelectrochemically is useful because (1) the liquid electrolyte establishes good contact with the entire surface of the cabbage-shaped CdTe rods and (2) photoexcited charge carriers are generated exclusively in the cabbage-shaped CdTe rods. Therefore, this work also provides a cost-effective technology and architectures suitable for the fabrication of solid-state photovoltaic cells with interpenetrating heterojunctions on the nanoscale level and high-efficiency photoelectrochemical solar cells. The excellent photovoltaic performance and its array-on-Ni configuration make them a promising candidate for applications in solar energy conversion devices.

Conclusions

In this work we study the structural, composition and photovoltaic performance of as-deposited CdTe thin films as a function of surfactant CTAB concentration during growth and post-deposition. Various highly crystalline CdTe structures could be obtained at a room temperature with a simple electrochemical deposition method. This is a fast, simple and reproducible method which does not require any template, catalyst or surfactant, but can synthesize various CdTe structures with basic or complex.

Meanwhile, it is also found that the concentration of CTAB have largely influenced the Cd and Te contents of the product. By increaseing of CTAB concentration, the as-deposited thin film changes from Te-rich to Cd-rich.

In addition, we find that cabbage-shaped CdTe array exhibited an improved open circuit voltage, short circuit current, fill factor, and consequently an overall enhancement of the power conversion efficiency than traditional CdTe nanorod array, so this structural may be beneficial for the potential applications in solar cells.

Our results presented here for their synthesis are a convenient platform where various morphologies of a variety of semiconductors on a conducting substrate are required. Meantime, it is believed that this synthetic approach can be used to synthesize other materials with controlling morphologies as required.

Acknowledgements

This work was financially supported by the Technology Development Program of Jilin Province (Grant No. 20100417) and National Natural Science Foundation of China (No. 51272086).

Notes and references

[a]*State key Laboratory of Superhard Materials, Jilin University, Changchun, 130012, PR China*
. Fax: +86-431-85168763; Tel: +86-431-85168763; E-mail: yanghb@jlu.edu.cn

[b]*Department of Physics and Chemistry, Heihe University, Heihe 164300, PR China*

† Electronic Supplementary Information (ESI) available: [details of any supplementary information available should be included here]. See DOI: 10.1039/b000000x/

‡ Footnotes should appear here. These might include comments relevant to but not central to the matter under discussion, limited experimental and spectral data, and crystallographic data.

1 Lewis, N. S. Science, 2007, 315, 798–801.
2 Service, R. F. Science, 2008, 319, 718–720.
3 Coakley, K. M.; McGehee, M. D. Chem. Mater, 2004, 16, 4533–4542.
4 Greene, L. E., Law, M.; Yuhas, B. D.; Yang, P. D. J. Phys. Chem. C, 2007, 111, 18451–18456.
5 Gur, I., Fromer, N. A., Geier, M. L., Alivisatos, A. P. Science ,2005,310, 462–465.
6 Chao Xie, Lin-Bao Luo, Long-Hui Zeng, Long Zhu, CrystEngComm, 2012, 14, 7222–7228
7 Sandeep Kumar and Thomas Nann, Chem. Commun, 2003, 2478–2479
8. Martin Schierhorn, Shannon W. Boettcher, Nano Lett, 2009, 9, 3262-3267.
9 Kayes, B. M., Atwater, H. A., Lewis, N. S. J. Appl. Phys, 2005, 97, 114302 1-11.
10 X.N. Wang, J. Wang, M.J. Zhou, H. Wang, X.D. Xiao, Q.Li, Journal of Crystal Growth , 2010, 312, 2310–2314
11 X. Wu, J.C. Keane, R.G. Dhere, C. Dehart, D.S. Albin, A. Duda, T.A. Gessert, S. Asher, D.H. Levi, P. Sheldon, in: Proceedings 17th European Photovoltaic Solar Energy Conference and Exhibition, Munich, 2001, p. 995
12 Bingwei Luo, Yuan Deng,* Yao Wang, Ming Tan, Lili Cao and Wei Zhu, CrystEngComm, 2012, 14, 7922–7928
13 J. L. Plaza, O. Martı´nez, S. Rubio, V. Hortelanob, E. Die´gueza, CrystEngComm, 2013, 15, 2314–2318
14 Xina Wang, Juan Wang, Minjie Zhou, J. Phys. Chem. C, 2009, 113, 16951–16953
15 Yun-Mo Sung, Woo-Chul Kwak, Tae Geun Kim, CrystEngComm, 2012, 14, 389–392
16 Parthiban Ramasamy, Shariful I. Mamum, Joonkyung Jang, CrystEngComm, 2013, 15, 2061–2066.
17 S. Ham, B. Choi, N. Myung, Journal of Electroanalytical Chemistry, 2007, 601, 77–82
18 Shu-Ying Yang , Jung-Chuan Chou , Herng-Yih Ueng. Thin Solid Films, 2009, 12, 077.
19 X.H. Ji, X.N. Song, J. Li, Y.B. Bai, W.S. Yang, X.G. Peng, J. Am. Chem. Soc. 2007, 129, 13939.
20 B.Q. Xie, Y.T. Qian, S.Y. Zhang, S.Q. Fu, W.C. Yu, Eur. J. Inorg. Chem. 2006, 12, 2454.
21 Y.D. Yin, A.P. Alivisatos, Nature. 2005, 437, 664.
22 Y.X. Wang, J. Sun, X.Y. Fan, X. Yu, Ceram. Int. 2011, 37, 3431.
23 A.P. de Moura, R.C. Lima, M.L. Moreira, D.P. Volanti, J.W.M. Espinosa, M.O.Orlandi, P.S. Pizani, J.A. Varela, E. Longo, Solid State Ionics. 2010, 18, 1775.
24 Xina Wang, Haojun Zhu, Yeming Xu, Hao Wang, ACS Nano, 2010, 4(6), 3302–3308.
25 Seong-Hun Kima, Wone-Keun Han, Jae-Ho Lee, Current Applied Physics, 2010, 10, S481–S483.
26 Zhu, L. P., Zhang, W. D., Xiao, H. M., Yang, Y. J. Phys. Chem. C, 2008, 112, 10073.
27 Wang, L. Z., Zhang, J. L., Chen, F., Anpo, M. J. Phys. Chem. C, 2007, 111, 13648.
28 Qianqian Shen, Jinbo Xue, Jian Liu, Husheng Jia, Xuguang Liubc, CrystEngComm, 2013, 15, 1007–1014
29 A. Fiore, R. Mastria, M. G. Lupo and G. Lanzani, J. Am. Chem. Soc., 2009, 131, 2274–2282.
30 Li L. Surfactant and Nanotechnology. Beijing: Chemical industry publishing, 2004.p. 83–8.
31 Lecheng Tian, Wuyou Fu, Minghui Li, CrystEngComm, 2012, 14, 4490–4495
32 Lei Fan and Rong Guo, Crystal Growth & Design, 2008, 8, 2150-2156.
33 X.N. Wang, J. Wang, Journal of Crystal Growth, 2010, 312, 2310–2314.
34 M. Schierhorn, S. W. Boettcher and A. Ivanovskaya, J. Phys. Chem. C, 2008, 112(23), 8516